CrossMark

SnS Thin Films Prepared by Chemical Spray Pyrolysis at Different Substrate Temperatures for Photovoltaic Applications

THIERNO SALL,[1] BERNABÉ MARÍ SOUCASE ⓘ,[1,2,3] MIGUEL MOLLAR,[1,2] and JUAN ANGEL SANS[1]

1.—Institut de Disseny i Fabricació, Universitat Politècnica de València, Camí de Vera s/n, 46022 Valencia, Spain. 2.—Departament de Física Aplicada, Universitat Politècnica de València, Camí de Vera s/n, 46022 Valencia, Spain. 3.—e-mail: bmari@fis.upv.es

The preparation and analysis of morphological, structural, optical, vibrational and compositional properties of tin monosulfide (SnS) thin films deposited on glass substrate by chemical spray pyrolysis is reported herein. The growth conditions were evaluated to reduce the presence of residual phases different to the SnS orthorhombic phase. X-ray diffraction spectra revealed the polycrystalline nature of the SnS films with orthorhombic structure and a preferential grain orientation along the (111) direction. At high substrate temperature (450°C), a crystalline phase corresponding to the Sn_2S_3 phase was observed. Raman spectroscopy confirmed the dominance of the SnS phase and the presence of an additional Sn_2S_3 phase. Scanning electron microscopy (SEM) images reveal that the SnS film morphology depends on the substrate temperature. Between 250°C and 350°C, SnS films were shaped as rounded grains with some cracks between them, while at substrate temperatures above 400°C, films were denser and more compact. Energy-dispersive x-ray spectroscopy (EDS) analysis showed that the stoichiometry of sprayed SnS films improved with the increase of substrate temperature and atomic force microscopy micrographs showed films well covered at 350°C resulting in a rougher and bigger grain size. Optical and electrical measurements showed that the optical bandgap and the resistivity decreased when the substrate temperature increased, and smaller values, 1.46 eV and 60 Ω cm, respectively, were attained at 450°C. These SnS thin films could be used as an absorber layer for the development of tandem solar cell devices due to their high absorbability in the visible region with optimum bandgap energy.

Key words: SnS, thin films, chemical spray pyrolysis, XRD, Raman spectroscopy, AFM, SEM, resistivity

INTRODUCTION

To obtain new photovoltaic materials to make solar cells cheaper and more efficient, tin monosulfide belonging to the IV–VI semiconductor group has gained much attention because of its suitable optoelectronic properties for photovoltaic applications. This compound has a direct bandgap near 1.3 eV,[1] which is close to the optimal band gap (1.5 eV) of solar cells and has a high absorption coefficient ($\alpha > 10^4$ cm^{-1}).[2] All SnS elements are abundant, cost-effective and less toxic compared to the cadmium and lead in CdS and PbS thin films, respectively. SnS also has p-type electrical conductivity, and it has a theoretical high efficiency greater than 24%,[3] but still, despite many efforts, solar cells based on SnS absorbers have not achieved conversion efficiency above 1.3% yet.[4] The low performance may be due to impurities and/or defects in the SnS layers that result from the preparation methods used. Tin monosulfide has been prepared using various techniques such as successive ionic

layer adsorption and reaction (SILAR),[5] chemical bath deposition (CBD),[6] electrochemical deposition (ECD),[7] Atomic layer deposition (ALD),[8] chemical spray pyrolysis (CSP),[9] etc. Each preparation technique has its own advantages and drawbacks, but the development of simple, rapid and economical methods for preparing materials with good reproducibility and with controllable deposition parameters is still a great challenge. We chose CSP for film deposition due to its inexpensive, swift, vacuumless, and simple preparation.[10] In addition, it is suitable for industrial scale production.

J. Malaquias et al. prepared SnS films on glass substrate using sulfurization of metallic precursors in an $N_2 + S_2$ atmosphere in a sulfurization temperature range from 300°C to 520°C. Solid mixtures of SnS, SnS_2 and Sn_2S_3 were obtained for all growth conditions, but optical and electrical measurements showed that the influence of secondary phases (SnS_2 and Sn_2S_3) was small compared to the SnS phase.[11] Sajeesh et al. deposited SnS by the CSP technique at varying substrate temperatures from 300°C to 500°C and found a prominent peak of the Sn_2S_3 phase at lower Ts (<300°C) and an SnS_2 phase above Ts (>400°C). Otherwise, no secondary phase was detected at 350°C.[12]

In this study, we prepared SnS thin films by the CSP technique onto simple glass substrates at different temperatures using a 1:1 ratio [S]/[Sn]. Some amount of alcohol (10%) was added to the aqueous solvent to reduce the water surface tension. The crystalline structure, morphology, chemical composition, electrical and optical properties of chemical spray pyrolysis deposited SnS thin films are reported.

EXPERIMENTAL DETAILS

Film Preparation

Tin monosulfide (SnS) thin films were prepared onto glass substrates from an aqueous solution containing tin (II) chloride dihydrate ($SnCl_2 \cdot 2H_2O$), thiourea ($CS(NH_2)_2$) (≥ 99%) and alcohol (10% in volume) to reduce the surface tension. The concentration of tin chloride was fixed at 0.104 M and the [S]/[In] ratio was 1. The substrate temperature varied: 250°C, 300°C, 350°C, 400°C, and 450°C. The volume sprayed was 5 mL, the spray rate was 1.5 mL/min, the air compressed pressure was 0.7 bar and the distance between the glass substrate and nozzle was kept at 25 cm.

Glass substrates were washed in an ultrasonic bath of acetone for 15 min, rinsed with distilled water followed by an ethanol bath for 15 min and rinsed with distilled water before drying and being used for the spray process.

Film Characterization

Structural properties were characterized by means of x-ray diffraction (XRD) measurement with a Rigaku Ultima IV diffractometer at the Bragg–Brentano ($\theta - 2\theta$) configuration, and using CuKα radiation (1.5418 Å). Phonon vibration properties were also characterized by Raman scattering measurements performed with a LabRAM HR UV spectrometer coupled to a Peltier-cooled CCD camera with a spectral resolution of 3 cm^{-1} and using a 632.81 nm laser excitation line. The morphology was characterized using JEOL-JSM6300 scanning electron microscopy (SEM) operating at 20 kV, and the atomic force microscopy (AFM) study was carried out using a Bruker Multimode 8 AFM Nanoscope V controller. Energy-dispersive x-ray spectroscopy (EDS) attached to scanning electron microscopy (SEM) was used for microanalysis. Sheet resistance was measured by the four-point probe technique and optical properties were monitored by transmittance using a Deuterium-Halogen lamp (DT-MINI-2-GS Micro Park) coupled to a 500 mm Yvon-Jobin HR460 spectrophotometer using a back-thinned Si-CCD detector (Hamamatsu) optimized for the UV–VIS-Infrared range.

RESULTS AND DISCUSSION

X-ray Diffraction (XRD) Analysis

Figure 1a shows the XRD spectra of SnS thin films sprayed at various substrate temperatures, i.e., 250°C, 300°C, 350°C, 400°C, and 450°C, respectively. From 250°C to 450°C the XRD peaks matched SnS orthorhombic phase (JCPDS#39-0354) well. XRD peaks were located at 26.10°, 30.47°, 31.53°, 39.05°, and 44.74°, corresponding to diffraction between the following crystallographic planes: (021), (101), (111), (131), and (141) respectively. The highest intensity observed for the (111) diffraction peak at 31.53° is the preferential crystallographic direction for all temperatures except for films prepared at 300°C in which the (101) peak dominates. Apart from the SnS peaks, one additional peak corresponding to the Sn_2S_3 phase was observed in the XRD spectra for films deposited at 450°C. This peak is due to the re-evaporation of SnS and tin from the substrate surface as vapor.[13] Sn_2S_3 is a compound made of SnS and SnS_2, which means that some Sn (IV) ions are present. This may happen if part of Sn (II) dismutates into Sn (0) and Sn (IV) to produce Sn_2S_3 as a secondary phase.[14,15] It is noteworthy to notice that at 400°C and 450°C, the (101) peak tends to vanish and simultaneously an increase of the (111) main peak is observed. A decrease of other indexed peaks at all temperatures below 400°C was also observed.

Figure 1b shows a detail of the XRD pattern around the (021), (101), and (111) peaks. It is noteworthy that the (111) peak at 400°C and 450°C is clearly the overlap of (101) and (111) observed at substrate temperatures between 250°C and 350°C.
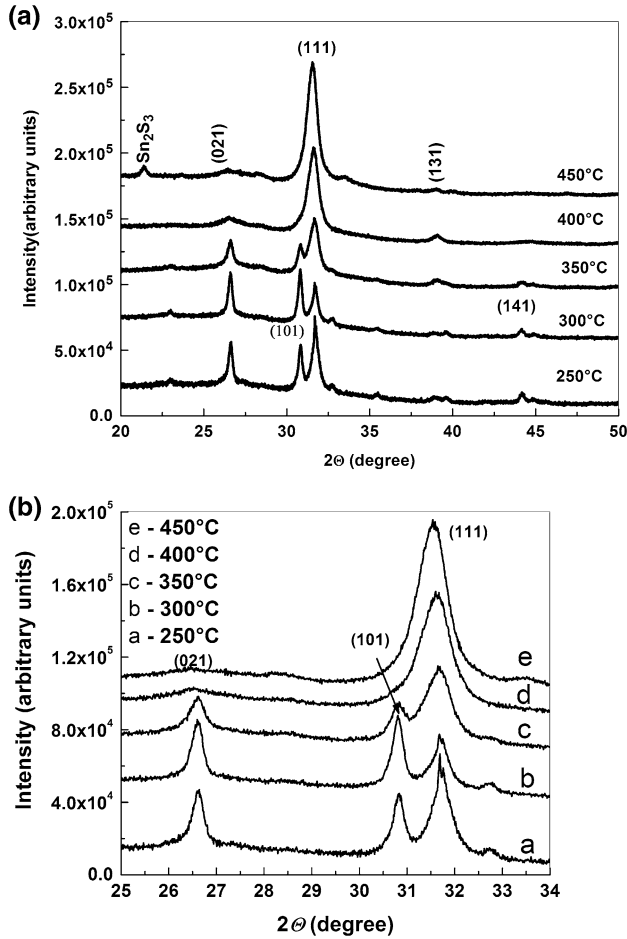
Fig. 1. (a) X-ray diffraction spectra of SnS films deposited by chemical spray pyrolysis at different substrate temperatures, (b) detail of the x-ray diffraction spectra of SnS films showing a zoom about the (111) peak.

The lattice plane index ($h\ k\ l$), interplanar distance d_{hkl} and lattice parameters have the following relationship for orthorhombic crystals[16]:

$$1/d_{hkl}^2 = h^2/a^2 + k^2/b^2 + l^2/c^2. \tag{1}$$

Using XRD data, we calculated the lattice parameters (a, b, and c) of SnS thin films. The evaluated lattice parameters of the SnS films are listed in Table I. Lattice parameters are in good agreement with the standard orthorhombic SnS pattern JCPDS#39-0354.

The variation of the crystallite size with substrate temperature was investigated using the Debye–Scherrer formula from the (111) and (101) diffraction lines after deconvolution of wide (111) peaks at 400°C and 450°C[17]:

$$D = K\lambda/\beta\cos\theta. \tag{2}$$

where β is the full width at half maximum (FWHM), λ wavelength of x-ray whose value is 1.5418 Å (CuKα), K the Scherrer constant, which generally

depends on the crystallite shape and is close to 1 ($K = 0.9$ was used) and θ is the Bragg angle at the center of the peak. The crystallite size, D, obtained from this equation corresponds to the mean minimum dimension of a coherent diffraction domain.

Table I shows the crystallite sizes calculated from the Scherrer's equation for (101) and (111) diffraction peaks. The trend is the higher the temperature the smaller the crystallite size and the higher the intensity. When the temperature increases, two competitive phenomena take place simultaneously: one is the increase of the crystallite size and the other one is the enlargement of the nucleation centers, which might result in an increase of the density of crystallites and then in an increase of the intensity of the diffraction peaks. In this case the second phenomenon is likely to dominate, and, as a result, a higher density of smaller crystallites is produced when the temperature increases.

Raman Spectroscopy Analysis

Raman spectroscopy is a powerful tool to analyze the phase and structure of SnS thin films. Raman spectra were analyzed to confirm the SnS phase and to identify the presence of the other phases as well. Raman spectra of SnS thin films deposited at different substrate temperatures recorded in the range 80–350 cm^{-1} are shown in Fig. 2. Raman spectroscopy reported modes for SnS at 94 cm^{-1}, 193 cm^{-1}, 218 cm^{-1}, and 225 cm^{-1} assigned to Ag, and 88 cm^{-1}, 170 cm^{-1}, and 178 cm^{-1} belonging to B2 g, and for Sn$_2$S$_3$ with a mode at 307 cm^{-1}.[11,18,19] The Raman mode at 307 cm^{-1} confirms the presence of the Sn$_2$S$_3$ phase for films deposited at 450°C, which is in good agreement with the XRD spectra in Fig. 1, in which the presence of the Sn$_2$S$_3$ for films deposited at 450°C and no Raman mode corresponding to SnS$_2$ were observed. Otherwise, Raman spectra also confirm that the SnS phase is obtained in all samples prepared at different temperatures. Therefore, both Raman and x-ray diffraction results were complimentary.

Scanning Electron Microscopy Analysis

An electron beam is used to scan the surface of films in the scanning electron microscope by applying a typical acceleration voltage of 20 kV. Scanning electron microscopy characterization was carried out on all samples, and representative micrographs are shown in Fig. 3. SEM studies revealed that the SnS thin films deposited from 250°C to 350°C substrate temperatures were well covered and strongly adherent to the glass surface with the formation of agglomerations of small grains probably formed due to the segregation of excess tin. At 400°C and 450°C SnS films were homogeneous, dense, pinhole free and more compact than films sprayed at lower temperatures. At lower temperatures (below 400°C), SnS grains had a spherical shape, being almost uniform and some voids

Table I. Crystallite sizes and lattice parameters of SnS films deposited at various substrate temperatures

Ts (°C)	Crystallite size (nm)		Lattice parameters (Å)		
	(101)	(111)	a	b	c
250	39.4	23.5	4.18	11.18	4.03
300	31.8	20.9	4.17	11.26	4.01
350	21.1	14.0	4.34	10.45	3.97
400	7.0	12.8	4.22	11.28	3.92
450	4.7	12.6	4.19	11.32	4.04
Standard-JCPDF#039-0354	–	–	4.32	11.19	3.98

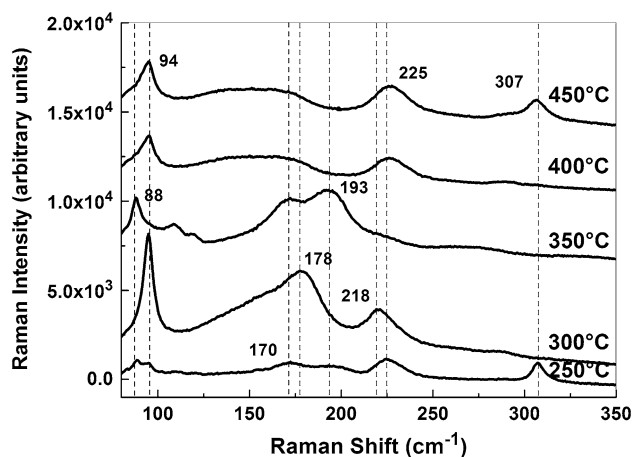Fig. 2. Raman spectra of SnS films deposited by chemical spray pyrolysis at different substrate temperatures.

Fig. 3. SEM images of SnS films deposited by chemical spray pyrolysis at different substrate temperatures.

between them were observed. At higher temperatures (at 400°C and 450°C), the grainy surface structure disappeared, and films were denser and more compact.

Atomic Force Microscopy Analysis

The surface topography of SnS films grown at different substrate temperatures was examined by atomic force microscopy and 2-D pictures scanning in an area of 3 μm×3 μm and a scale bar in the height of 70 nm are shown in Fig. 4. When the substrate temperature increased from 350°C to 450°C, the film surface roughness decreased from 24.7 nm to 16.6 nm probably due to the suppression of the segregation of tin on the surface. Films deposited at 350°C were the roughest (24.7 nm) and had the largest grain size (252 nm), while films prepared at 450°C had the lowest roughness (16.6 nm) and the smallest grain size (148 nm). Roughness and grain size for all samples are shown in Table II. Furthermore, when the substrate temperature increased from 350°C to 450°C, the void fraction over the surface decreased, resulting in a reduction of the roughness (Table II). Therefore, the film surfaces were smoother compared to films prepared at 250°C and 300°C. The difference
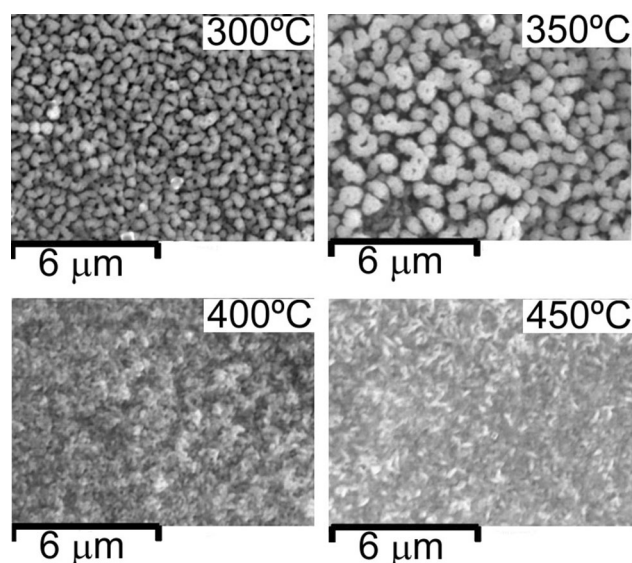
between the crystallite size given by Scherrer's equation and the grain size given by AFM is due to the fact that a grain is an agglomeration of several crystallites.

Taken into account the data provided by XRD and AFM measurements, the increase of substrate temperature results in the formation of a larger number of crystallites but with smaller sizes. This effect can be related to the generation of a higher density of nucleation centers with the temperature resulting in a higher density of crystallites but with smaller sizes.

Energy-Dispersive X-ray Spectroscopy Measurements

Energy-dispersive x-ray spectroscopy is a powerful technique to analyze the chemical composition of the sample, being based on x-rays emitted by the atoms in the sample. The molar ratios shown in Table III indicate that all films contain only sulfur and tin. The proportion of S and Sn in SnS thin films revealed that when the substrate temperature
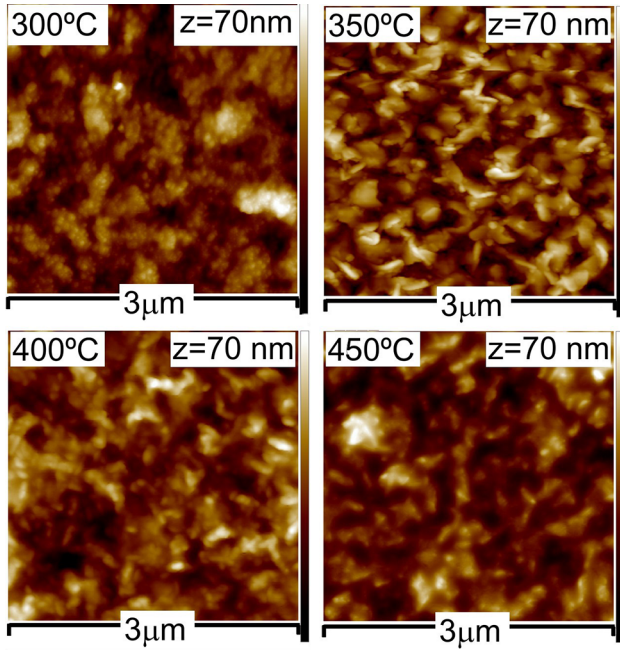
Fig. 4. AFM micrographs of SnS films deposited by chemical spray pyrolysis at different substrate temperatures.

Table II. Roughness and grain size of SnS films prepared at various substrate temperatures

Ts (°C)	Roughness (nm)	Grain size (nm)
250	20.6	174
300	17.3	219
350	24.7	252
400	21.5	177
450	16.6	148

Table III. Composition of SnS films deposited onto glass substrate obtained by EDS at different temperatures

Ts (°C)	%Sn	%S	S/Sn
250	56.4	43.6	0.77
300	56.1	43.9	0.78
350	55.3	44.7	0.81
400	53.3	46.7	0.88
450	52.6	47.4	0.90

increased from 250°C to 350°C, all the ratios indicated an excess of tin, but when the substrate temperature was 400°C and 450°C, respectively, a drastic decrease in the amount of tin was observed, leading to S/Sn close to unity, confirming the XRD results. Therefore, according to the EDS results, the stoichiometry deviation can be attributed to the excess of tin.

Table IV. Thickness and resistivity measurements of SnS films deposited onto glass substrates at different temperatures

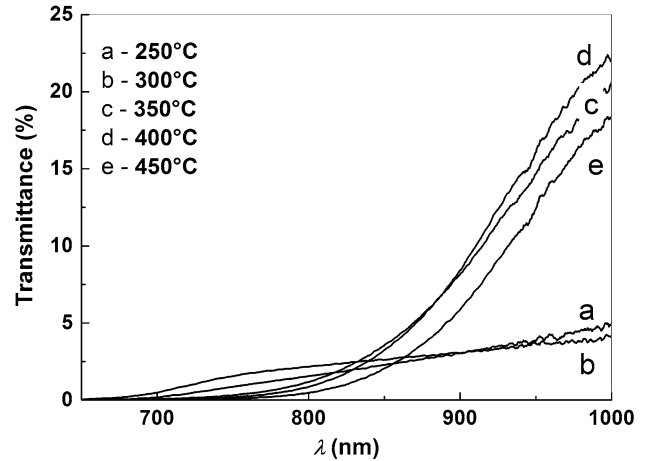| Samples	Thickness (nm)	Slope	R^2 (Ω)	ρ (Ω cm)
250	1530	0.25×10^7	1.13×10^7	1695
300	1350	0.20×10^7	0.90×10^7	1215
350	1090	0.18×10^7	0.81×10^7	883
400	912	0.13×10^7	0.58×10^7	529
450	576	0.23×10^6	1.04×10^6	60

Fig. 5. Optical transmission spectra of SnS films deposited with different substrate temperatures.

Electrical Measurements

The resistivity of the samples was obtained by the four-probe technique. Table IV displays the thickness, sheet resistance, and resistivity of all samples in relation to the substrate temperature. A decrease in the resistivity of films was observed when the substrate temperature rose from 250°C to 450°C, being correlated with the decrease of film thicknesses. The lowest thickness (576 nm) and resistivity (60 Ω cm) were obtained for films prepared at the highest temperature, 450°C.

Optical Analysis

The optical transmittance of SnS thin films deposited by CSP onto simple glass taken in the range of 500–1000 nm is displayed in Fig. 5. We noted a low transmittance at low substrate temperature of 250°C and an increase of the transmittance from 300°C to 450°C due to the decrease of thickness when the substrate temperature increased from 250°C to 450°C. We also noted, particularly, that films prepared at a substrate temperature in the range of 350°C to 450°C had the same transmittance variation. For all films, the transmittance
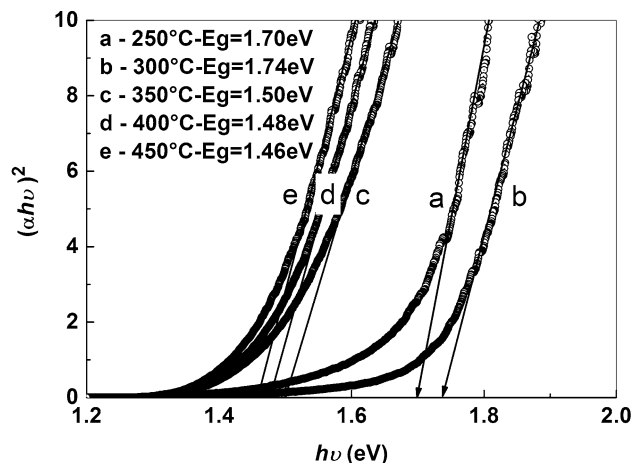
Fig. 6. Plot of $(Ah\nu)^2$ versus the photon energy ($h\nu$) of SnS thin films prepared at different substrate temperatures.

starts above 800 nm, as characteristic for an SnS absorber layer.

The bandgap energies for SnS thin films were obtained from optical transmission data plotting $(Ah\nu)^2$ versus $h\nu$ at various temperatures, where A is the absorbance and $h\nu$ is the photon energy. The calculated optical bandgap for every sample appears in the legend of Fig. 6. At lower temperatures, 250°C and 300°C, a suitable bandgap energy between 1.70 eV to 1.74 eV was calculated, while at a higher substrate temperature, in the range of 350°C to 450°C, the gap energy decreased from 1.50 eV (the ideal bandgap energy) to 1.46 eV. The change in preferred film orientation from (010) to (111) planes can be correlated to the change in the optical gap energy of SnS thin films; the optical bandgap of SnS changed from 1.74 eV to 1.46 eV when the substrate temperature increased from 300°C to 450°C, respectively, where the parallel plane was replaced by a plane perpendicular to the surface.

CONCLUSIONS

Tin monosulfide (SnS) thin films were deposited by the CSP technique using $SnCl_2 \cdot 2H_2O$ and $CS(NH_2)_2$ as precursors of tin (II) and sulfur, respectively. All films were polycrystalline and crystallized in the SnS orthorhombic phase, with (111) as the main peak. No SnS_2 Raman mode was observed, while Sn_2S_3 modes were detected, thus confirming the XRD results. In addition, two SnS modes were observed in all samples. The SnS films showed a granular morphology between 250°C and 350°C, while at 400°C and 450°C, films became denser and more compact. According to energy-dispersive x-ray spectroscopy results, films with improved stoichiometry could be achieved with higher substrate temperatures, and AFM micrographs showed films with a greater roughness and relatively big grain size. The optical energy bandgap and electrical resistivity were found to decrease with the increase of the substrate temperature achieving a minimum of 1.46 eV and 60 Ω cm at 450°C, respectively.

Polycrystalline SnS films with good stoichiometry, denser and compact morphology and suitable gap energy of 1.46–1.50 eV were obtained by the CSP inexpensive technique and also using abundant elements (Sn and S), making SnS to be a promising candidate to substitute the $CuInS_2$ absorber layer in solar cells thin films technology.

The results obtained herein emphasize that the influence of substrate temperatures on the physical and chemical properties of pyrolysised SnS films is crucial in order to produce suitable SnS films, which have to be deposited at temperatures from 350°C to 450°C.

REFERENCES

1. N.R. Mathews, H.B.M. Anaya, M.A. Cortes-Jacome, C. Angeles-Chavez, and J.A. Toledo-Antonio, *J. Electrochem. Soc.* 157, H337 (2010).
2. N. Koteeswara Reddy, K. Ramesh, R. Ganesan, K. Reddy, K.R. Gunasekhar, and E. Gopal, *Appl. Phys. A* 83, 133 (2006).
3. J.J. Loferski, *J. Appl. Phys.* 27, 777 (1956).
4. K.T.R. Reddy, N.K. Reddy, and R.W. Miles, *Sol. Energy Mat. Sol. C* 90, 3041 (2006).
5. C. Gao, H.L. Shen, L. Sun, H.B. Huang, L.F. Lu, and H. Cai, *Mater. Lett.* 64, 2177 (2010).
6. D. Avellaneda, M.T.S. Nair, and P.K. Nair, *J. Electrochem. Soc.* 155, D517 (2008).
7. J.R.S. Brownson, C. Georges, and C. Levy-Clement, *Chem. Mater.* 19, 3080 (2007).
8. P. Sinsermsuksakul, J. Heo, W. Noh, A.S. Hock, and R.G. Gordon, *Adv. Eng. Mat* 1, 1116 (2011).
9. T. Sall, M. Mollar, and B. Marí, *J. Mater. Sci.* 51, 7607 (2016).
10. K. Otto, A. Katerski, O. Volobujeva, A. Mere, and M. Krunks, *Energy Proc.* 3, 63 (2011).
11. J. Malaquias, P.A. Fernandes, P.M.P. Salomé, and A.F. da Cunha, *Thin Solid Films* 519, 7416 (2011).
12. T.H. Sajeesh, A.R. Warrier, C. Sudha Kartha, and K.P. Vijayakumar, *Thin Solid Films* 518, 4370 (2010).
13. M. Vasudeva Reddy, G. Sreedevi, C. Park, R.W. Miles, and K.T. Ramakrishna Reddy, *Curr. Appl. Phys.* 15, 588 (2015).
14. A. Molenaar, *Extended Abstracts,* vol. 84-2, Pennington, N.J., 634 (1984).
15. S. López, S. Granados, and A. Ortiz, *Semicond. Sci. Technol.* 11, 433 (1996).
16. B. Cullity, *Elements of X-ray Diffraction* (New York: Addision-Wesley Publishing Company Inc, 1967), p. 501.
17. G. Willeke, R. Dasbach, B. Sailer, and E. Bucher, *Thin Solid Films* 213, 271 (1992).
18. H.R. Chandrasekhar, R.G. Humphreys, U. Zwick, and M. Cardona, *Phys. Rev. B* 15, 2177 (1977).
19. S. Cheng and G. Conibeer, *Thin Solid Films* 520, 837 (2011).